

Andrzej WOŹNIAKOWSKI<sup>1</sup>, Józef DENISZCZYK<sup>1</sup>

# STABILITY PHASE DIAGRAM OF THE Ir-Pt SOLID SOLUTION – NUMERICAL MODELLING FROM FIRST PRINCIPLES

First principles based numerical methods are used to determine the phase stability diagram of the Ir-Pt solid solution with  $A_1$ -type crystal structure. Ising-like cluster expansion formalism was used to construct the lattice Hamiltonian. Phase diagram was calculated with the use of Monte Carlo simulations. Miscibility gap in this system was predicted. Calculated consolute temperature ( $T_C$ ) is about 1250 K at 50% of platinum when excess vibrational contribution to the free energy was included. The result is in good quantitative agreement with experimental data.

## 1. INTRODUCTION

Platinum group metals (*PGMs* - ruthenium, rhodium, palladium, osmium, iridium, platinum) and their alloys are widely used in many industrial applications, such as: electronics, automotive, aerospace or medicine because of their excellent physical and chemical properties. *PGMs* can be used at extremely high temperatures under mechanical loads and simultaneous corrosive attack [15], [18].

Key properties that make platinum and its alloys uniquely suitable for biomedical applications are its inertness and biocompatibility, high mechanical strength and corrosion resistance. Platinum and platinum alloys are used in a wide range of medical devices such as heart pacemakers, cardioverter defibrillators and catheters which can be inserted inside the body. Pacemakers which are used to treat heart disorders, usually contain at least two platinum-iridium electrodes, through which pulses of electricity are transmitted to stabilise the heartbeat. Also an implantable cardioverter defibrillators components are made from platinum or (*PGMs*) alloys, such as platinum-iridium wires for multi-pin hermetic seal or Pt-Ir alloy rings for shocking electrodes [7].

Pure platinum (Pt) crystallizes in  $A_1$  (face centered cubic – fcc) structure and has melting point at 2041 K. Near the room temperature lattice constant of Pt is 0.39236 nm. Same as platinum, iridium (Ir) exists in face centered cubic structure and has the highest melting point (at 2719 K) from the metals which belong to platinum group metals. The lattice constant of iridium at 293 K is 0.38392 nm [2]. Platinum alloys with 10–20% of iridium are used in production of medical components because of their biocompatibility, strength and corrosion resistance [18].

The first ( $T$ - $x$ ) phase diagrams of the Ir-Pt system were proposed by E. Raub [16] and S.R. Bhardawaj and S.N. Tripathi [3]. In the both studies miscibility gaps were obtained but with different values of consolute temperature and at different critical concentrations of platinum:  $T_C = 1249$  K at 60% Pt [16] and  $T_C = 1643$  K at 25% Pt [3]. The miscibility gap was also observed using electrical resistivity

<sup>1</sup>Institute of Materials Science, University of Silesia, ul. 75 Pułku Piechoty 1A, 41-500 Chorzów, Poland.

measurements [14]. In recent years the ( $T$ - $x$ ) phase diagram of the  $\text{Ir}_{1-x}\text{Pt}_x$  alloy was the subject of experimental and theoretical studies [8], [26]. The results presented in ref. [26] suggest that there are no evidence from the metallurgical experiments for existence of the miscibility gap in the Ir–Pt system. Opposite to the reported experimental data, thermodynamic calculations which were performed in the same studies suggest presence of the miscibility gap in the  $\text{Ir}_{1-x}\text{Pt}_x$  alloy, but it should be noted, that any systematic ground state search for this system was not performed [26].

The present work aims to extend the study of phase stability of the Ir–Pt system. Based on our earlier experience, [24], [25] and many others studies [1], [5], [6], we are convinced that is possible to calculate the ( $T$ - $x$ ) phase diagram very close to the experimental results with the use of *ab-initio* method supplemented with the Monte Carlo (*MC*) simulations. The knowledge of the correct phase boundaries might be very helpful in preparation of the  $\text{Ir}_{1-x}\text{Pt}_x$  alloy.

The outline of the paper is as follows. In Section 2 we describe the computational details. Section 3 presents the results of the *ab initio* calculations of the formation enthalpies, results of the ground state search and phase diagram calculations of the Ir–Pt system. Conclusions are presented in Section 4.

## 2. COMPUTATIONAL DETAILS

The alloy formation energies, which are basic quantities in the cluster expansion approach, defined as:

$$\Delta E_f = E_{\text{Ir}_{1-x}\text{Pt}_x} - xE_{\text{Pt}} - (1-x)E_{\text{Ir}},$$

were calculated with the use of the Vienna *ab initio* Simulation Package *VASP* [10], [11], [12], [13] implementing the Blöchl's projector augmented wave approach [4], with the generalized gradient approximation for exchange and correlation potentials. The pseudopotentials with the valence electron configurations,  $\text{Ir-}s^1d^8$  and  $\text{Pt-}s^1d^9$ , were applied. Total energy calculations were converged with respect to gamma centered k-point sampling. A plane-wave energy cutoff of 500 eV was used which yields  $\Delta E$  values that are converged to within a few meV per atom. Electronic degrees of freedom were optimized with a conjugate gradient algorithm, and both cell constant and ionic positions were fully relaxed.

The first principles phase diagram calculations were performed based on the *VASP* results. All remaining steps were done using Alloy Theoretic Automated Toolkit (*ATAT*) package [19], [20], [21]. In the first step the calculated energies were used to construct cluster expansion (*CE*) [17] Hamiltonian in a form of polynomial in the Ising-like occupation variables:

$$\Delta E(\sigma) = \sum_{\alpha} m_{\alpha} J_{\alpha} \langle \prod_{i \in \alpha'} \sigma_i \rangle,$$

where  $\alpha$  is a cluster defined as a set of lattice sites,  $m_{\alpha}$  indicate the number of clusters that are equivalent by symmetry to  $\alpha$  divided by the number of lattice sites. The sum is taken over all clusters  $\alpha$  that are not equivalent by a symmetry operation and the average is taken over all clusters  $\alpha'$  that are equivalent to  $\alpha$  by symmetry. The information regarding the energetics of the alloy are embodied in coefficients  $J_{\alpha}$  which are called the Effective Cluster Interaction (*ECI*). The predictive ability of the cluster expansion is controlled by the Cross Validation Score (*CVS*):

$$CVS = \left( \frac{1}{n} \sum_{i=1}^n (E_i - \hat{E}_{(i)})^2 \right)^{\frac{1}{2}},$$

where  $E_i$  is *ab initio* calculated formation energy of superstructure  $i$ , while  $\hat{E}_{(i)}$  represents the energy of superstructure  $i$  obtained from *CE* with the use of the remaining  $(n-1)$  structural energies. It worth note, that typical well-converged cluster expansion system required calculation of the formation energy for 30-50 ordered superstructures and contains 10-20 *ECI* parameters.

Contributions of lattice vibrations to the free energies were introduced employing the coarse-graining formalism [22]. For each superstructure the vibrational free energy was calculated within the harmonic approximation. To reduce the computational time needed for obtaining phonon densities for a large set

of superstructures the bond-length-dependent transferable force constant approximation was used [22]. In the last step, the phase diagram calculations were performed with the use of the Monte Carlo (MC) thermodynamic integration within the semi-grand-ensemble [21].

### 3. RESULTS AND DISCUSSION

*Ab initio* VASP calculations of the ground state energy were performed for the end-member elements Ir and Pt and for the formation energies of 36 superstructures representing the  $\text{Ir}_{1-x}\text{Pt}_x$  alloy with different composition  $x$ . The optimal number of superstructures were determined by minimizing the cross-validation score between *ab initio* computations and the cluster expansion prediction. The resulting CVS is about 6.5 meV/atom. Our detailed search for the structures with negative ground-state formation enthalpy failed what indicates presence of the miscibility gap in this system. Figure 1 is a plot of formation energies calculated with the use of the VASP and predicted by CE. In Figure 1 the green

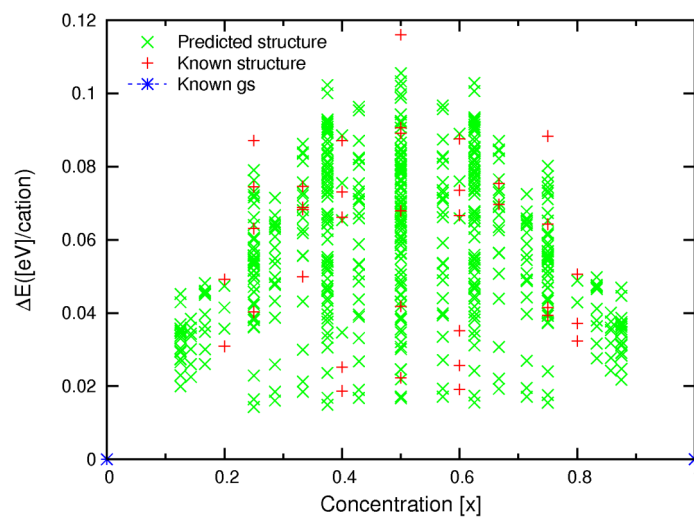


Fig. 1. Formation energies of  $\text{Ir}_{1-x}\text{Pt}_x$  calculated by VASP (red cross) and predicted by cluster expansion (CE) (green cross).

stars are predicted candidates for the intermediate ground states. We have analysed about 593 possible structures. Of course only few of them from each concentration were calculated with the use of *ab-initio* VASP method (red crosses): two structures at 20% platinum were calculated, four at 25% of Pt, another four at 33% of Pt, five at 40%, in a half way to iridium six structures were calculated, six at 60% of Pt, two at about 67%, four at 75% and three structures at 80 percent of platinum. The blue stars represent known end-member Ir and Pt ground states, and there are no other ground states found within the superstructures consisting of up to 8 atoms per unit cell. All supercell energies are positive what means the presence of miscibility gap and is consistent with experimental phase diagrams which were obtained by E. Raub [16] and S.R Bhardawaj and S.N. Tripathi [3].

Resulted from the fitting procedure ECI parameters are plotted as a function of inter-atomic separations in Figure 2. Fitting procedure of CE, controlled by CVS parameter, gave the cluster expansion CE including only pairs interaction parameters, what strongly suggest presence of the strictly symmetric miscibility gap in this system. It is evident that with increasing distance between sites of cluster the values of pair ECI falls down in an oscillatory manner. Low value of cross validation score (CVS) and decreasing magnitudes of the ECI confirmed quality of our calculations and suggest convergence of the cluster expansion (CE) in this system.

Figure 3 shows the calculated phase stability diagram for the Ir–Pt system in  $A_1$  (fcc) crystal structure. Resulting temperature independent ECI were used to calculate the lower solvii (blue line). The upper solvii (red line) represents calculations based on temperature dependent ECI which imply the inclusion of excess vibrational contributions to the free energy.

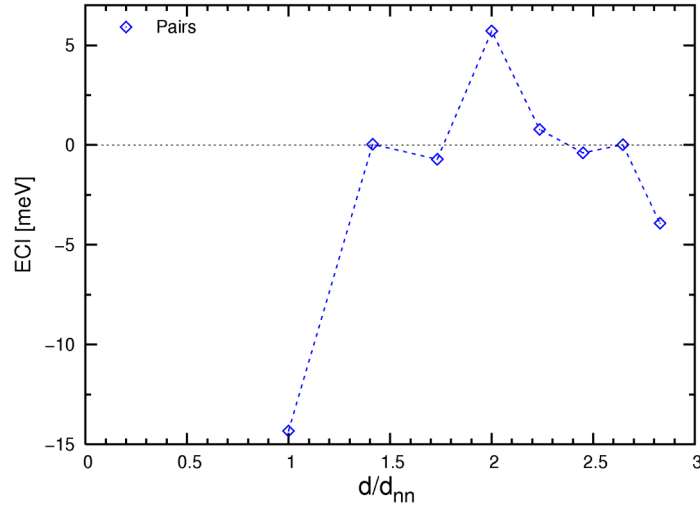


Fig. 2. Pair effective cluster interactions ( $ECI$ ) as a function of inter-atomic distance expressed in units of the nearest neighbor distance ( $d_{nn}$ )

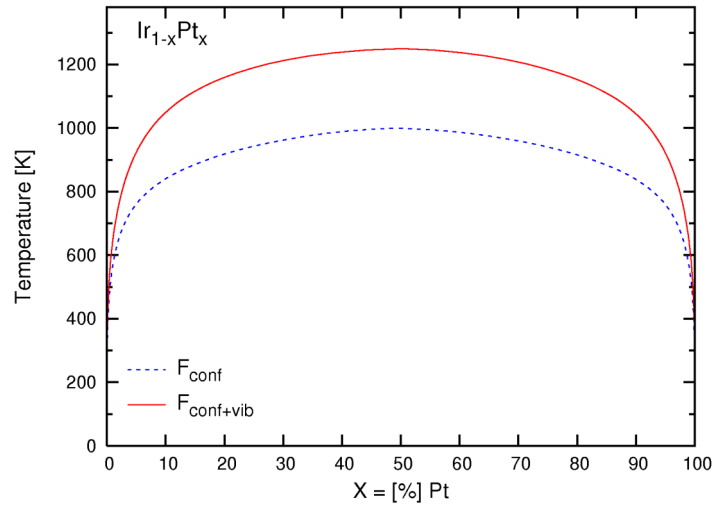


Fig. 3. Modelled phase stability diagram for the  $Ir_{1-x}Pt_x$  solid solution. Blue and red lines show respectively the diagram based on the  $ECI$  fitted to the configuration formation enthalpy and on the temperature-dependent  $ECI$  fitted to the sum of configuration and vibration free energy.

Our main result is the calculated consolute temperature ( $T_C$ ) which is about 1000K at 50% platinum when only the configurational degrees of freedom are taken into account and 1250K at 50% platinum obtained on the basis of temperature dependent  $ECI$  what is in good quantitative agreement with experimental data reported in [16]. It is worth to note that in most miscibility gap systems inclusion of the excess vibrational contributions to the free energy leads to reduction in consolute temperature ( $T_C$ ), nevertheless similar enhancement of  $T_C$  occurs in CdSe-CdS with wurtzite and zincblende crystal structures [24]. We have shown [24] that the inclusion of temperature-dependent  $ECI$  increases the calculated consolute temperatures ( $T_C$ ). The effect was also discussed in ref. [9], [23].

#### 4. CONCLUSIONS

Systematic ground state search for the  $Ir_{1-x}Pt_x$  alloy was performed with the use of cluster expansion ( $CE$ ) method. There are no intermediate ground states predicted in our expansion. As we expected, based on our formation energies calculations and obtained Effective Cluster Interactions ( $ECI$ ), strictly symmetric miscibility gap was predicted. Calculated consolute point is  $(T_C, x_C) = (1000 \text{ K}, 0.50)$

when only the configurational part of free energy is considered and (1250 K, 0.50) when the excess free energy due to lattice vibrations is also taken into account. It is worth to note, that inclusion of vibrations increases the consolute temperature by 25% (similarly as reported in [24] for the CdSe-CdS system). Our research supports experimental results reported by E. Raub ( $T_C = 1249$  K,  $x_C = 0.60$ ) [16].

## BIBLIOGRAPHY

- [1] ADJAOUD O., STEINLE-NEUMANN G., BURTON B.P., VAN DE WALLE A., First-principles phase diagram calculations for the HfC-TiC, ZrC-TiC and HfC-ZrC solid solutions, *Phys. Rev. B*, 2009, Vol. 80, pp. 134112.
- [2] BEDFORD R.E., BONNIER G., MAAS H., PAVESE F., Recommended values of temperature on the International Temperature Scale of 1990 for a selected set of secondary reference points, *Metrologia*, 1996, Vol. 33 (2), pp. 133.
- [3] BHARDAWAJ S.R., TRIPATHI S.N., The Ir-Pt (Iridium-Platinum) System, *J. Phase Equil.*, 1995, Vol. 16, pp. 460.
- [4] BIÖCHL P.E., Projector augmented-wave method, *Phys. Rev. Lett. B*, 1994, Vol. 50, pp. 17953.
- [5] BURTON B.P., van de Walle A., First principles phase diagram calculations for the system NaCl-KCl: The role of excess vibrational entropy, *Chemical Geology*, 2006, Vol. 225, pp. 222.
- [6] BURTON B.P., VAN DE WALLE A., KATTNER U., First principles phase diagram calculations for the wurtzite structure systems AlN-GaN, GaN-InN, and AlN-InN, *J. Appl. Phys.*, 2006, Vol. 100, pp. 113528.
- [7] COWLEY A., WOODWAR B., A Healthy Future: Platinum in Medical Applications. Platinum group metals enhance the quality of life of the global population, *Platinum Metals Rev.*, 2011, Vol. 55, pp. 98.
- [8] FRANKE P., NEUSCHUTZ D., Ir-Pt (Iridium – Platinum), Binary Systems. Part 5: Binary Systems Supplement 1, Landolt-Bornstein – Group IV Physical Chemistry, 2007, Vol. 19B5, pp. 1.
- [9] GARBULSKY G.D., CEDER G., Contribution of the vibrational free energy to phase stability in substitutional alloys: Methods and trends, *Phys. Rev. B*, 1996, Vol. 53, pp. 8993.
- [10] KRESSE G., HAFNER J., Ab initio molecular dynamics for liquid metals, *Phys. Rev. B*, 1993, Vol. 47, pp. 558-561.
- [11] KRESSE G., HAFNER J., Ab initio molecular simulation of the liquid-metal–amorphous-semiconductor transition in germanium, *Phys. Rev. B*, 1993, Vol. 49, pp. 14251.
- [12] KRESSE G., FURTHMÜLLER J., Efficiency of ab-initio total energy calculations for metals and semiconductors using a plane-wave basis set, *Comput. Mat. Science*, 1996, Vol. 6, pp. 15.
- [13] KRESSE G., FURTHMÜLLER J., Efficient iterative schemes for ab initio total-energy calculations using a planewave basis set, *Phys. Rev. Lett.*, 1996, Vol. 54, pp. 11169.
- [14] MASING G., ECKHARDE K., KLOIBER K., *Z. METALLK.*, 1940, Vol. 32, pp. 122.
- [15] MERKER J., LUPTON D., TOPFER M., KNAKE H., High Temperature Mechanical Properties of the Platinum Group Metals, Elastic Properties of Platinum, Rhodium and Iridium and Their Alloys at High Temperatures, *Platinum Metals Review*, 2001, Vol. 45, pp. 74.
- [16] RAUB E., Metals and alloys of the platinum group, *J. Less Common Met.*, 1959, Vol. 1, pp. 3.
- [17] SANCHEZ J.M., DUCASTELLE F., GRATIAS D., Generalized cluster description of multicomponent systems, *Physica A*, 1984, Vol. 128, pp. 334.
- [18] VAITHINATHAN K., LANAM R., Features and Benefits of Different Platinum Alloys, Technical Articles: Alloys, Platinum Guild International, USA, 2005: <http://www.platinumguild.com/output/page2414.asp>.
- [19] VAN DE WALLE A., CEDER G., Automating first principles phase diagram calculations, *J. Phase Equil.*, 2002, Vol. 23, pp. 348.
- [20] VAN DE WALLE A., ASTA M., CEDER G., The alloy theoretic automated toolkit: A user guide, *Calphad*, 2002, Vol. 26, pp. 539.
- [21] VAN DE WALLE A., ASTA M., Self-driven lattice-model Monte Carlo simulations of alloy thermodynamic, *Modelling Simul. Mater. Sci. Eng.*, 2002, Vol 10, pp. 521.
- [22] VAN DE WALLE A., CEDER G., The effect of lattice vibrations on substitutional alloy thermodynamics, *Rev. Mod. Phys.*, 2002, Vol. 74, pp. 11.
- [23] VAN DE WALLE A., CEDER G., Automating first principles phase diagram calculations, *J. Phase Equil.*, 2002, Vol. 23, pp. 348.
- [24] WOŹNIAKOWSKI A., DENISZCZYK J., ADJAOUD O., BURTON B.P., First principles phase diagram calculations for the CdSe-CdS wurtzite, zincblende and rock salt structures, *Comp. Meth. Mater. Sci.*, 2013, Vol. 13, pp. 345.
- [25] WOŹNIAKOWSKI A., DENISZCZYK J., Phase diagram calculations for the ZnSe – BeSe system by first-principles based thermodynamic Monte Carlo integration, *Comp. Meth. Mater. Sci.*, 2013, Vol. 13, pp. 351.
- [26] YAMABE-MITARAI Y., AOYAGI T., ABE T., An investigation of phase separation in the Ir-Pt binary system, *J. Alloys Comp.*, 2009, Vol. 484, pp. 327.